frontiers in Materials

ORIGINAL RESEARCH
published: 25 May 2021
doi: 10.3389/fmats.2021.682833

Energy Down-Conversion $Cs_3Cu_2Cl_5$ Nanocrystals for Boosting the Efficiency of UV Photodetector

Chengjun Liu[1,2†], Lixi Wang[2†], Fan Fang[2], Zihan Zhao[2], Jiangyong Pan[3], Javed Akram[4], Suhaidi Bin Shafie[5], Razika Zair Talaighil[6], Qing Li[2], Zhiwei Zhao[2], Jun Wu[2], Zhuoya Zhu[2], Wei Lei[2]*, Xiaobing Zhang[2]* and Jing Chen[2]**

[1] State Key Laboratory of Nuclear Power Safety Monitoring Technology and Equipment, China Nuclear Power Engineering Co., Ltd., Shenzhen, China, [2] Joint International Research Laboratory of Information Display and Visualization, School of Electronic Science and Engineering, Southeast University, Nanjing, China, [3] School of Electronic and Information Engineering, Nanjing University of Information Science and Technology, Nanjing, China, [4] COMSATS University Islamabad, Islamabad, Pakistan, [5] Institute of Advanced Technology, Universiti Putra Malaysia, Serdang, Malaysia, [6] Research Unit of Materials Processes and Environment (URMPE), University M'hamed Bougara of Boumerdes, Boumerdes, Algeria

OPEN ACCESS

Edited by:
Subbiah Thirumaran,
Annamalai University, India

Reviewed by:
He Huang,
Soochow University, China
Tsung-Rong Kuo,
Taipei Medical University, Taiwan

***Correspondence:**
Jiangyong Pan
pjy@nuist.edu.cn
Wei Lei
lw@seu.edu.cn
Xiaobing Zhang
bell@seu.edu.cn
Jing Chen
chenjing@seu.edu.cn

[†] These authors have contributed equally to this work

Specialty section:
This article was submitted to Colloidal Materials and Interfaces, a section of the journal Frontiers in Materials

Received: 19 March 2021
Accepted: 13 April 2021
Published: 25 May 2021

Citation:
Liu C, Wang L, Fang F, Zhao Z, Pan J, Akram J, Shafie SB, Talaighil RZ, Li Q, Zhao Z, Wu J, Zhu Z, Lei W, Zhang X and Chen J (2021) Energy Down-Conversion $Cs_3Cu_2Cl_5$ Nanocrystals for Boosting the Efficiency of UV Photodetector. Front. Mater. 8:682833. doi: 10.3389/fmats.2021.682833

Zero-dimension (0-D) lead halide perovskite nanocrystals (NCs) have attracted a sight of interest in the field of optoelectronic devices due to their outstanding properties, such as high photoluminescence quantum yield (PLQY) and size- and composition-controlled tunable emission wavelengths. However, the toxicity of lead (Pb) element in the lead perovskite NCs is the bottleneck for the commercial application of perovskite NCs. Herein, we report a facile ligand-assisted synthesis to achieve lead-free $Cs_3Cu_2Cl_5$ NCs with a high PLQY of ~70% and good stability against environmental oxygen/moisture as a promising down-conversion material. It has good merits of high PLQY and large Stokes shift (~300 nm) originated from the effect of Jahn–Teller distortion and self-trapped excitons (STEs). Furthermore, the $Cs_3Cu_2Cl_5$ NCs embedded composite films (NCCFs) were utilized to enhance the ultraviolet (UV) response of silicon (Si) photodetectors. External quantum efficiency (EQE) measurements show that the UV response can be greatly improved from 3.3 to 19.9% @ 295 nm based on NCCFs combined with Si photodiodes. Our work offers an effective approach to develop highly efficient and stable lead-free $Cs_3Cu_2Cl_5$ NCs for the application in the solar-blind UV photodetector.

Keywords: lead-free perovskite, all-inorganic perovskite nanocrystals, photoluminescence quantum yield, ligand-assisted, stability

INTRODUCTION

In the field of photodetection, silicon-based photodetectors have achieved great progress on account of their broadband spectral response, high responsivity, and cost-effective fabrication process, while the response of silicon-based photodetectors in the ultraviolet (UV) region has been limited by the shallow penetration depth of UV radiations (less than 20 nm @370 nm wavelength) and high reflection coefficient (An et al., 2013). One strategy is to enhance the UV detection of Si photodetectors by down-conversion materials such as all-inorganic lead halide perovskite nanocrystals (NCs) that transform the UV photons to visible lights (Zhang et al., 2018).

A good down-conversion layer needs to display high light absorption in the UV wavelength, good quantum yield, extraordinary transparency in the visible region, and large Stokes shift to reduce the self-reabsorption losses. Moreover, structural simplicity, low-cost fabrication, ambient operation, and long-term stability are also crucial figures of merit for real applications (Wang et al., 2017).

The origin of the Stokes shift is closely related to the excitonic finestructure, which consists of a manifold of closely spaced optical transitions arising from the quasi-degenerate bandedge electronic states (Voznyy et al., 2016), leading to the down-conversion phenomenon of the nanocrystals (NCs). However, the relatively small Stokes of lead halide perovskite NCs' shift brings about significant self-reabsorption loss. Moreover, the toxicity of lead (Pb) element in the lead perovskite NCs is the bottleneck for the commercial application of perovskite NCs (Chang et al., 2018). Recently, the work of lead-free perovskite NCs, including tin-based (Jellicoe et al., 2016; Wang et al., 2016; Zhang et al., 2016; Wang et al., 2017; Liang et al., 2020) and bismuth-based (Leng et al., 2016, 2018; Yang et al., 2017; Bekenstein et al., 2018; Zhou et al., 2018; Gao et al., 2019) perovskite NCs, has been targeted. Replacing lead with divalent non-toxic metal cations (e.g., tin and bismuth) or heterovalent metal cations (e.g., antimony and silver) has been developed to synthesize lead-free perovskite NCs. Unfortunately, the rapid oxidation of Sn^{2+} to Sn^{4+} in air is detrimental to the photoluminescence quantum yield (PLQY) (Jellicoe et al., 2016; Wang et al., 2016, 2017; Zhang et al., 2016, 2017; Bekenstein et al., 2018; Chang et al., 2018; Leng et al., 2018; Zhou et al., 2018; Gao et al., 2019; Liang et al., 2020; Pan et al., 2020b). Therefore, it is of great interest to exploit novel NCs with lower toxicity and higher stability, especially for larger Stokes shift as down-conversion materials.

The copper halide NCs, such as $Cs_3Cu_2X_5$ (X = Cl, Br, and I) with large Stokes shift (∼300 nm) and high PLQY in visible spectrum but sensitivity to UV radiation as well as excellent photo stability, appear to be ideal candidates as down-conversion materials for the UV photodetection application (Yang et al., 2018; Cheng et al., 2019; Li et al., 2020; Lian et al., 2020a,b; Luo et al., 2020; Wang et al., 2020). The tetrahedral structure of $Cs_3Cu_2X_5$ can be formed by Cu^+ coordinated with halide ions, which is different from octahedral structure of lead halide perovskite NCs (Pan et al., 2016, 2020a; Yang et al., 2018; Cheng et al., 2019; Li et al., 2020; Wang et al., 2021). Meanwhile, $Cs_3Cu_2X_5$ NCs exhibit strong emission of self-trapped excitons (STEs), originating from the excited-state structural deformation and possesses (Wang et al., 2018, 2019; Cheng et al., 2019; Li et al., 2020; Lian et al., 2020a). Moreover, the photoluminescence (PL) of $Cs_3Cu_2X_5$ NCs exhibits distinct redshift while adjusting the halide ions from I^- to Cl^- (Lian et al., 2020a). As reported, stable and deep-blue emissive $Cs_3Cu_2I_5$ NCs with high PLQY (∼87%) were synthesized via hot-injection method. Encouraged by the remarkable efficiency of $Cs_3Cu_2I_5$ NCs, the proposed LEDs (∼445 nm) showed an external quantum efficiency (EQE) of ∼1.21% comparable to that of blue LEDs based on lead halide perovskite (Wang et al., 2020). In addition, it is reported that zero-dimension (0-D) $Cs_3Cu_2I_5$ NCs with a PLQY of 73.7% acted as sensitive X-ray scintillators for the application of X-ray imaging (Lian et al., 2020b). Despite these great efforts, to the best of our knowledge, there is no report about efficient and stable UV photodetectors based on $Cs_3Cu_2X_5$ NCs.

Herein, we report lead-free and all-inorganic $Cs_3Cu_2Cl_5$ NCs synthesized by a facile hot-injection method, whose PL peak is located at 525 nm with a high PLQY of ∼70%. Meanwhile, the 0-D $Cs_3Cu_2Cl_5$ NCs by ligand-assisted passivation show large Stokes shift (∼300 nm), long lifetime, and considerable stability against air humidity. The $Cs_3Cu_2Cl_5$ QDs embedded composite films (NCCFs) with high transparency and PLQY were fabricated onto the front side of the Si photodetectors to extend the response range to the solar-blind UV region of 257–300 nm, and the EQE was increased from 3.3 to 19.66% @295 nm.

EXPERIMENT SECTION

Materials

Cesium carbonate (Cs_2CO_3, 99.9%), oleylamine (OAm, 80–90%), *n*-hexane (AR), and isopropanol (AR) were purchased from Macklin, cuprous chloride (CuCl, ≥99.95%) was purchased from Aladdin, oleic acid (OA, 90%) was purchased from Aldrich, and 1-octadecene (ODE, ≥90%) was purchased from General-Reagent. All of the chemicals were used as received without further purification.

Preparation of Cs-Oleate

0.3258 g of Cs_2CO_3, 6.84 mL of 1-octadecene, and 3.16 mL of oleic acid were loaded into a 50-mL three-neck flask and dried for 1 h at 110°C, and then heated to 120°C under N_2 until all Cs_2CO_3 reacted with OA. The precursor has to be pre-heated to 100°C before injection.

Synthesis of $Cs_3Cu_2Cl_5$

In a typical synthesis of $Cs_3Cu_2Cl_5$ NCs, 0.1188 g of CuCl, 2 mL of OA, and 1 mL of OAm were mixed in a 50-mL three-neck flask and degassed under vacuum for 1 h at 110°C. After complete solubilization of CuCl, the temperature was raised to 160°C and kept for 5 min. Then, 6 mL of Cs-oleate solution was quickly injected and, 5 s later, the reaction mixture was cooled with an ice-water bath. The solution was filtrated by 0.22-μm filter and then centrifuged at 6,000 rpm for 5 min. After centrifugation, the supernatant was discarded and the precipitate was dissolved in the mixture of n-hexane and isopropanol (1:1 by volume). The mixture was centrifuged at 600 rpm for 5 min to collect the precipitants.

Preparation of QDs Embedded Organic Polymer Film

The $Cs_3Cu_2Cl_5$ NCs powder was dispersed in the mixture of polydimethylsiloxane (PDMS) and curing agent (10:1 by weight), followed by heating at 90°C for 3 h under vacuum. For the fabrication of NCs embedded modified polyester (Ecoflex) film, $Cs_3Cu_2Cl_5$ NCs solution was mixed with polyester and stirred intensely. The QDs embedded film was obtained after static positioning for 30 min at room temperature in air.

Characterization

Absorption and PL spectra of QDs were measured by using the U-4100 and NIR-300 spectrophotometers, respectively. PLE, PLQY, and TRPL spectra were measured by an Edinburgh instruments FS5 spectrometer. Transmission electron microscopic (TEM) image of QDs was taken by the Tecnai G20. Si photodiodes were purchased from Beijing Light Sensing Technologies Ltd., part number LSSPD-5.9. The photoresponse of the detectors was characterized by Keithley 2400 source meter.

RESULTS AND DISCUSSION

The tunneling electron microscopic (TEM) image shows that $Cs_3Cu_2Cl_5$ NCs have a mean size of 3.4 nm with uniform size distribution (**Figure 1A**). Moreover, the clear lattice fringes are observed in the high-resolution TEM (HRTEM) image, indicating the good crystallinity of NCs (**Figure 1B**). The X-ray diffraction (XRD) patterns in **Figure 1C** confirm that the crystal phase of the obtained NCs coincides with the standard PXRD data of $Cs_3Cu_2Cl_5$. Both the characterization results of TEM and XRD confirm the successful synthesis of the lead-free $Cs_3Cu_2Cl_5$ NCs. As shown in **Figure 1D**, the $Cs_3Cu_2Cl_5$ NCs adopt an orthorhombic space group Pnma (Lian et al., 2020a). There are two types of Cu^+ sites in this crystal that form $[Cu_2Cl_5]^{3-}$ units, namely, a tetrahedral site and a triangular site. The framework of $Cs_3Cu_2Cl_5$ NCs consists of $[Cu_2Cl_5]^{3-}$ that are separated by Cs^+ cations (Luo et al., 2020).

We further investigated the photophysical properties of $Cs_3Cu_2Cl_5$ NCs. **Figure 2A** reveals that the photoluminescence (PL) peak of $Cs_3Cu_2Cl_5$ NCs is located at 525 nm, while the absorbance peak is located at 225 nm, indicating a relatively large exciton binding energy, consistent with previous reports (Li et al., 2020; Lian et al., 2020a). We improved the PLQY of $Cs_3Cu_2Cl_5$ NCs by optimizing the quantities of OAm during the synthesis. The QY of NCs is improved from 5.6 to 69.1% when the volume of OAm is increased from 1 to 2 mL, which is consistent with the variation of PL intensity (**Figure 2B**). The time-resolved PL (TRPL) decay spectra of $Cs_3Cu_2Cl_5$ NCs were performed to gain a deep insight into the exciton recombination dynamics. As shown in **Supplementary Figure 2** and **Supplementary Table 1**, the lifetime of $Cs_3Cu_2Cl_5$ NCs is improved from 77.8 to 119.8 μs when the volume of OAm is increased from 1 to 2 mL. The prolonged exciton lifetime indicates the suppression of non-radiative recombination. Furthermore, the radiative and non-radiative decay rates were calculated based on the PLQY and the average lifetimes. The non-radiative recombination rate of 2 mL OAm is the lowest, quantitatively manifesting that non-radiative recombination can be suppressed by appropriate OAm. Broad emission with a long lifetime is a characteristic of

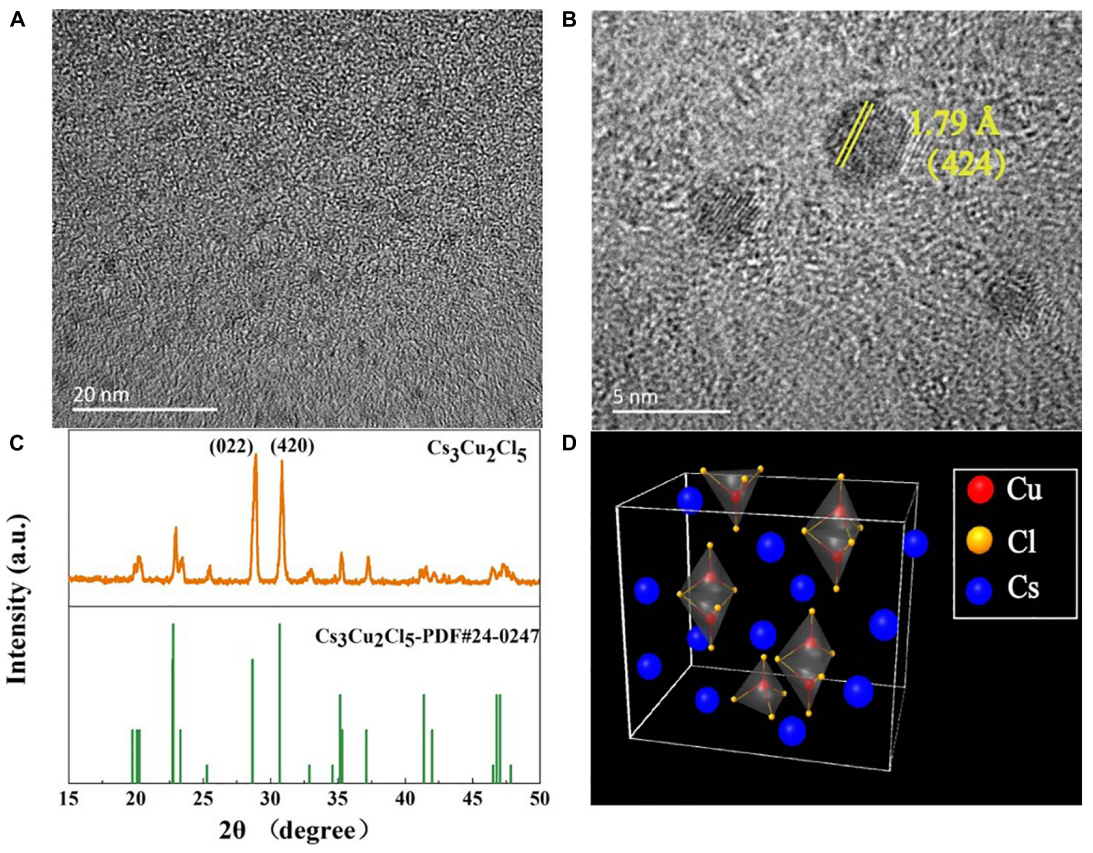

FIGURE 1 | (A) TEM image of $Cs_3Cu_2Cl_5$ NCs. **(B)** HRTEM image of $Cs_3Cu_2Cl_5$ NCs. **(C)** XRD pattern of $Cs_3Cu_2Cl_5$ NCs. **(D)** Crystal structure of $Cs_3Cu_2Cl_5$.

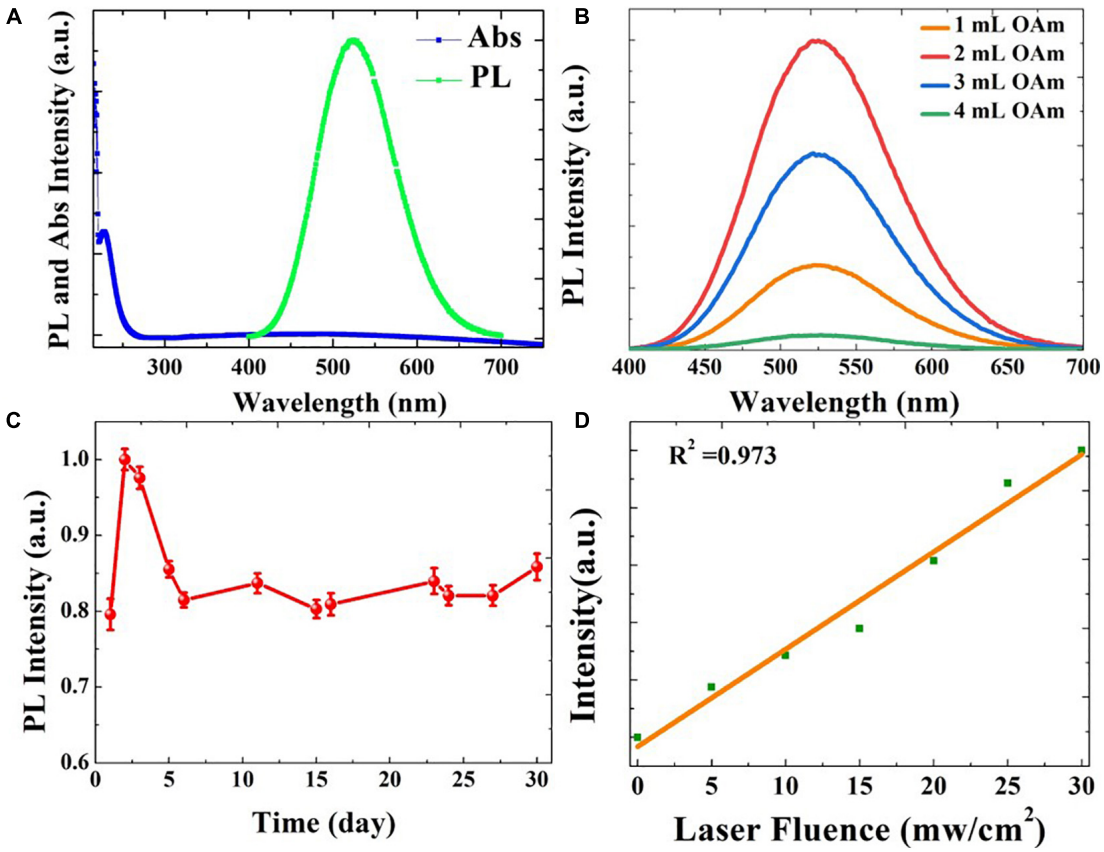

FIGURE 2 | (A) PL and absorption spectra of $Cs_3Cu_2Cl_5$ NCs solution. **(B)** PL spectra of different quantities of OAm-capped NCs. **(C)** Air-stability test of $Cs_3Cu_2Cl_5$ NCs. **(D)** Dependence of the emission intensity in $Cs_3Cu_2Cl_5$ NCs.

Cu(I)-complexed PL emissions involving Jahn–Teller distortion. And the Stokes shift is determined primarily by the energy difference between Cu(I)$3d^{10}$ and Cu(II)$3d^9$ (Jun et al., 2018). The stability of the $Cs_3Cu_2Cl_5$ NCs was measured under ambient environment and the PL intensity can be remained 85% of the initial intensity after 30 days (**Figure 2C**). The decrease of the PL intensity may be attributed to the aggregation of the NCs in the colloidal solution or the oxidation of Cu^+ to Cu^{2+} on the NCs' surface (Lian et al., 2020b). It is noted that the PL intensity of NCs has an obvious enhancement after 24 h, ascribing to the passivation of surface defect states by water molecules.

To shed light on the emission mechanism of $Cs_3Cu_2Cl_5$ NCs, the relationship between the emission and the excitation intensity is characterized to explore whether the PL emission is originated from permanent defects. As shown in **Figure 2D**, the PL intensity increases linearly with the increment of the excitation intensity, without saturation of PL, indicating that the PL emission arises from the intrinsic emitting states of material other than the permanent defect (Lian et al., 2020a). We also measured the emission wavelength-dependent photoluminescent excitation (PLE) spectra and excitation wavelength-dependent PL spectra of $Cs_3Cu_2Cl_5$ NCs. The normalized PLE spectra kept the uniform shapes with different detected emission wavelengths ranging from 480 to 580 nm. Similarly, the normalized PL spectra kept the identical features when the excitation wavelength increased from 250 to 340 nm (**Supplementary Figure 3**). Such uniform features of PLE and PL spectra with different detected emission or excitation wavelengths reveal that the green PL emission of $Cs_3Cu_2Cl_5$ NCs originates from the relaxation of the same excited states instead of ion luminescence. All the characterizations above indicate that the STEs obviously dominate the emission mechanism of the $Cs_3Cu_2Cl_5$ NCs.

Considering that the transmittance of NCCFs is vital for the performance of photodetectors coated with NCCFs, the transmittance of different organic polymer films was investigated. **Figure 3A** shows that the PDMS films are highly transparent with an average transmittance of 70% @400–800 nm, while the transmittance of modified polyester (Ecoflex) films decreases almost linearly from 44.48% @800 nm to 16.5% @ 400 nm. **Figure 3B** shows that the PL and Absorbance spectra of NCCFs are consistent with those of NCs, indicating that the superior optical property of $Cs_3Cu_2Cl_5$ NCs is well preserved. The high PLQY, good transmittance, and outstanding stability make NCCFs an attractive candidate for down-conversion application to enhance the UV detection of Si photodetectors. As shown in **Figure 3C**, the NCCFs were directly coated onto the surface of the Si photodiode, covering the whole detection area. The

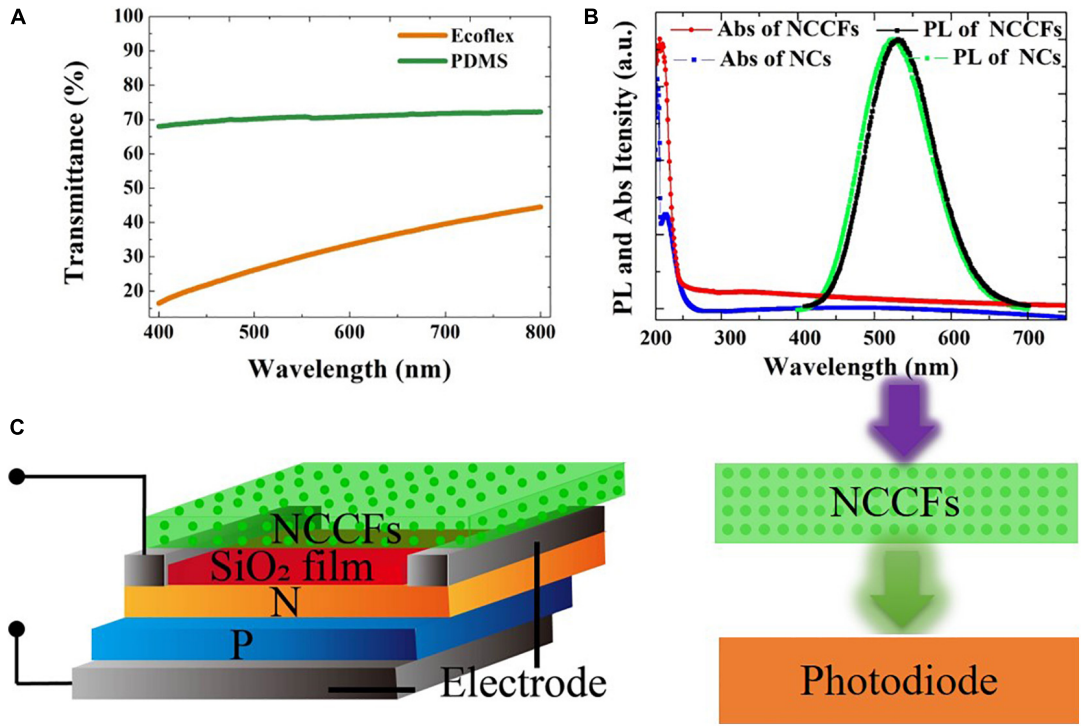

FIGURE 3 | (A) Transmittance spectra of the Ecoflex and PDM. **(B)** Abs spectra and PL spectra of $Cs_3Cu_2Cl_5$ NCs and NCCFs. **(C)** Schematic diagram of the configuration of the UV-enhanced Si photodiode and the down-conversion process of NCCFs.

enhancement of UV detection of the Si photodetector with NCCFs can be analyzed by considering the light converting progress as displayed in the right of **Figure 3C**. The incident photons with energy above the bandgap of the NCCFs can be transformed to visible photons by the down-conversion of film due to the high PLQY of $Cs_3Cu_2Cl_5$ NCs. Then most of the visible photons can pass through the NCCFs, followed by reception by the Si detector.

Subsequently, we characterized the Si photodetector coated with NCCFs to evaluate the effect of $Cs_3Cu_2Cl_5$ NCs on device performance. The photoresponsivity (R), specific detectivity (D^*), and external quantum efficiency (EQE) are evaluated according to the following equations (Li et al., 2017):

$$R = \frac{I_p - I_d}{P \cdot S} \tag{1}$$

$$D^* = \frac{A^{1/2}R}{(2eI_d)^{1/2}} \tag{2}$$

$$\mathrm{EQE} = \frac{I_p/e}{P/h\upsilon} = R\frac{hc}{e\lambda} \tag{3}$$

Where I_p, I_d, S, A, h, and c is the photocurrent, dark current, effective illuminated area, detection area, Planck's constant, and light speed, respectively.

The EQE characteristics reveal that the bare Si photodetector was not sensitive to UV radiation ranging from 257 to 300 nm, while the response of the NCCFs-coated Si photodetector can be extended to 257 nm (**Figure 4A**). The maximum EQE of the NCCFs-coated Si photodetector achieves 19.66% @295 nm compared with 3.3% of the bare photodetector, indicating the efficient down-conversion of NCCFs for the Si photodetector. The EQE reduction of the photodetector in the visible spectrum can be ascribed to the limited transmittance of NCCFs and the self-absorption-induced loss. As shown in **Figure 4B**, the letter "U" was imaged by the NCCFs-coated Si photodetector equipped with a slide rail controlled by a stepping motor.

The response speed is a key parameter for a photodetector that reflects the stability to catch a fast-transforming optical signal. We used a signal generator to generate incident light with different frequencies and recorded the photocurrent through an oscilloscope in real time. The current–time (I–T) curves of the NCCFs-coated Si photodetector are recorded under the incident light with the frequency ranging from 100 to 3,000 Hz (**Figure 4C** and **Supplementary Figure 5**). It is obvious that the NCCFs-coated Si photodetector can operate at a relatively wide frequency with outstanding stability and reproducibility. The relative balance $[(I_{max} - I_{min})/I_{max}]$ of the NCCFs-coated Si photodetector is maintained at 97.2% at a frequency of 3,000 Hz which indicates the potential application at high frequency and capacity to monitor ultrafast optical signals (Yan et al., 2019; Yu et al., 2019). Moreover, on the condition of 1,000 Hz incident light, the rise time of the device (from 10 to 90% of the saturated value) is about 28 μs, while the decay time is 40 μs (from 90 to 10%), indicating the fast response speed of the device (**Figure 4D**).

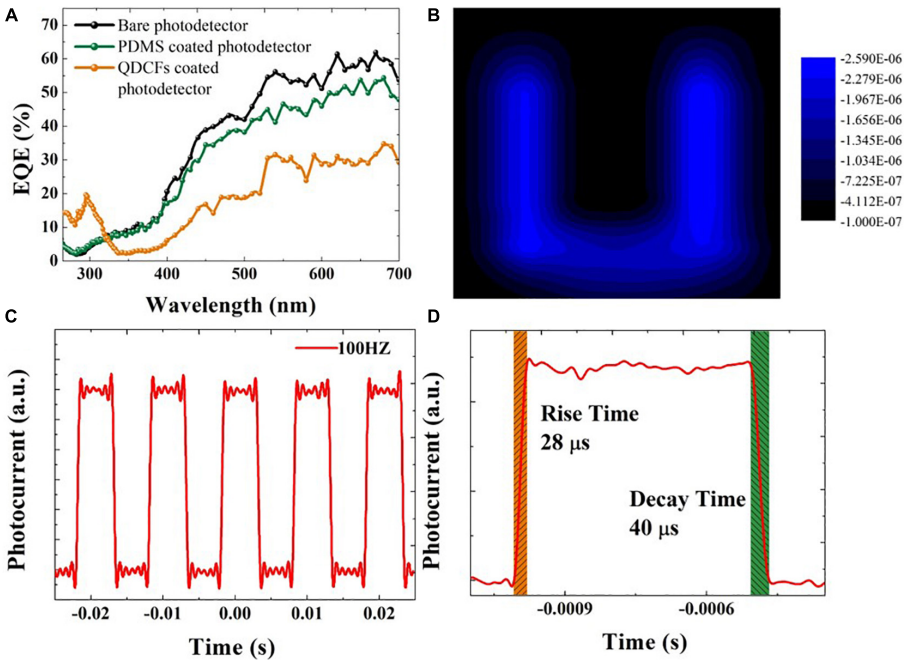

FIGURE 4 | (A) EQEs of bare, PDMS-coated, and NCCFs-coated Si photodiodes. **(B)** Imaging of the letter U. Photoresponse characteristics of the NCCFs-coated Si photodiodes to pulse light irradiation at frequencies of **(C)** 100 Hz. **(D)** Rising and decaying edges of one response cycle for estimating the response time of the photodetector.

CONCLUSION

In conclusion, 0-D colloidal $Cs_3Cu_2Cl_5$ NCs have been successfully synthesized via a hot-injection method. The prepared $Cs_3Cu_2Cl_5$ NCs exhibit a high PLQY of ~70% with the PL peak located at 525 nm, a large Stokes shift, and an extremely long lifetime, which is attributed to the STEs' effect. Moreover, the as-prepared NCs exhibited excellent air stability over 30 days. These features make them very suitable for down-conversion applications. By applying the NCCFs on to the top of the Si photodetector, we successfully fabricated the prototype devices of solar-blind UV-enhanced Si photodetectors. The NCCFs-coated Si photodiodes extended the response spectra to UV region of 257–300 nm and improved the EQE from 3.3 to 19.66% @295 nm. Our work offers an effective and low-cost approach to achieve UV-enhanced Si photodetectors toward broadband and solar-blind light detection.

DATA AVAILABILITY STATEMENT

The original contributions presented in the study are included in the article/**Supplementary Material**, further inquiries can be directed to the corresponding author/s.

AUTHOR CONTRIBUTIONS

WL and JP led the device physics work. JC led the materials chemistry work. CL synthesized and optimized the QD materials and carried out the device fabrication and characterizations. ZhZ and FF conducted the optical measurements and analyzed the optical properties of QDs. CL and LW wrote the first draft of the manuscript. JC, WL, XZ, and JP provided major revisions. JC and WL supervised the project. All authors discussed the results and commented on the manuscript.

FUNDING

This work was supported by the State Key Laboratory of Nuclear Power Safety Monitoring Technology and Equipment (K-A2020.415), National Key Research and Development Program of China (2018YFE0125500 and 2016YFB0401600), Program 111_2.0 in China (BP0719013), National Natural Science Foundation Project of China (61775034, 51879042, 61674029, and 12005038), Research Fund for International Young Scientists (62050410350), International Cooperative Research Project of Jiangsu Province (BZ2018056), Leading Technology of Jiangsu Basic Research Plan (BK20192003), Natural Science Foundation of Jiangsu Province (BK20190774), and Postgraduate Research and Practice Innovation Program of Jiangsu Province (KYCX19_0082).

SUPPLEMENTARY MATERIAL

The Supplementary Material for this article can be found online at: https://www.frontiersin.org/articles/10.3389/fmats.2021.682833/full#supplementary-material

REFERENCES

An, X., Liu, F., Jung, Y. J., and Kar, S. (2013). Tunable graphene-silicon heterojunctions for ultrasensitive photodetection. *Nano Lett* 13, 909–916. doi: 10.1021/nl303682j

Bekenstein, Y., Dahl, J. C., Huang, J., Osowiecki, W. T., Swabeck, J. K., Chan, E. M., et al. (2018). The Making and Breaking of Lead-Free Double Perovskite Nanocrystals of Cesium Silver-Bismuth Halide Compositions. *Nano Letters* 18, 3502–3508. doi: 10.1021/acs.nanolett.8b00560

Chang, Y. H., Lin, J. C., Chen, Y. C., Kuo, T. R., and Wang, D. Y. (2018). Facile synthesis of two-dimensional Ruddlesden-Popper perovskite quantum dots with fine-tunable optical properties. *Nanoscale Res Lett* 13, 247.

Cheng, P., Sun, L., Feng, L., Yang, S., Yang, Y., Zheng, D., et al. (2019). Colloidal Synthesis and Optical Properties of All-Inorganic Low-Dimensional Cesium Copper Halide Nanocrystals. *Angew Chem Int Ed Engl* 58, 16087–16091. doi: 10.1002/anie.201909129

Gao, M. Y., Zhang, C., Lian, L., Guo, J., Xia, Y., Pan, F., et al. (2019). Controlled synthesis and photostability of blue emitting Cs3Bi2Br9 perovskite nanocrystals by employing weak polar solvents at room temperature. *Journal of Materials Chemistry C* 7, 3688–3695. doi: 10.1039/c9tc00400a

Jellicoe, T. C., Richter, J. M., Glass, H. F. J., Tabachnyk, M., Brady, R., Dutton, S. E., et al. (2016). Synthesis and Optical Properties of Lead-Free Cesium Tin Halide Perovskite Nanocrystals. *Journal of the American Chemical Society* 138, 2941–2944.

Jun, T., Sim, K., Iimura, S., Sasase, M., Kamioka, H., Kim, J., et al. (2018). Lead-Free Highly Efficient Blue-Emitting Cs3 Cu2 I5 with 0D Electronic Structure. *Adv Mater* 30, e1804547.

Leng, M., Chen, Z., Yang, Y., Li, Z., Zeng, K., Li, K., et al. (2016). Lead-Free, Blue Emitting Bismuth Halide Perovskite Quantum Dots. *Angewandte Chemie-International Edition* 55, 15012–15016.

Leng, M., Yang, Y., Zeng, K., Chen, Z., Tan, Z., Li, S., et al. (2018). All-Inorganic Bismuth-Based Perovskite Quantum Dots with Bright Blue Photoluminescence and Excellent Stability. *Advanced Functional Materials* 28, 1704446. doi: 10.1002/adfm.201704446

Liang, H., Yuan, F., Johnston, A., Gao, C., Choubisa, H., Gao, Y., et al. (2020). High Color Purity Lead−Free Perovskite Light−Emitting Diodes via Sn Stabilization. *Advanced Science.* 7, 1903213. doi: 10.1002/advs.201903213

Li, Y., Vashishtha, P., Zhou, Z., Li, Z., Shivarudraiah, S. B., Ma, C., et al. (2020). Room Temperature Synthesis of Stable, Printable Cs3Cu2X5 (X = I, Br/I, Br, Br/Cl, Cl) Colloidal Nanocrystals with Near-Unity Quantum Yield Green Emitters (X = Cl). *Chemistry of Materials* 32, 5515–5524. doi: 10.1021/acs.chemmater.0c00280

Li, Y., Shi, Z. F., Li, S., Lei, L. Z., Ji, H. F., Wu, D., et al. (2017). High-performance perovskite photodetectors based on solution-processed all-inorganic CsPbBr3 thin films. *Journal of Materials Chemistry C* 5, 8355–8360. doi: 10.1039/c7tc02137b

Lian, L., Zheng, M., Zhang, P., Zheng, Z., Du, K., Lei, W., et al. (2020a). Photophysics in Cs3Cu2X5 (X = Cl, Br, or I): Highly Luminescent Self-Trapped Excitons from Local Structure Symmetrization. *Chemistry of Materials* 32, 3462–3468. doi: 10.1021/acs.chemmater.9b05321

Lian, L., Zheng, M., Zhang, W., Yin, L., Du, X., Zhang, P., et al. (2020b). Efficient and Reabsorption-Free Radioluminescence in Cs3Cu2I5 Nanocrystals with Self-Trapped Excitons. *Adv Sci (Weinh)* 7, 2000195. doi: 10.1002/advs.202000195

Luo, Z., Li, Q., Zhang, L., Wu, X., Tan, L., Zou, C., et al. (2020). 0D Cs3 Cu2 X5 (X = I, Br, and Cl) Nanocrystals: Colloidal Syntheses and Optical Properties. *Small* 16, e1905226.

Pan, J., Zhao, Z., Fang, F., Wang, L., Wang, G., Liu, C., et al. (2020b). Multiple Cations Enhanced Defect Passivation of Blue Perovskite Quantum Dots Enabling Efficient Light−Emitting Diodes. *Advanced Optical Materials.* 8, 1.

Pan, J., Chen, J., Huang, Q., Khan, Q., Liu, X., Tao, Z., et al. (2016). Size Tunable ZnO Nanoparticles To Enhance Electron Injection in Solution Processed QLEDs. *ACS Photonics* 3, 215–222. doi: 10.1021/acsphotonics.5b00267

Pan, J., Fang, F., Xie, J., Wang, L., Chen, J., Chang, J., et al. (2020a). Synergistic effects of charge transport engineering and passivation enabling efficient inverted perovskite quantum-dot light-emitting diodes. *Journal of Materials Chemistry C* 8, 5572–5579. doi: 10.1039/d0tc00661k

Voznyy, O., Fan, F., Ip, A., Kiani, A., Thon, S. M., Kemp, K. W., et al. (2016). Passivation-sensitive exciton finestructure produces excess 251 Stokes shifts in colloidal quantum dots. *arXiv [preprint]* arXiv:1608.05113,

Wang, Q., Zhang, X., Orcid, Z. J., Zhang, J., Gao, Z., Li§Orcid, Y., et al. (2017). Energy-Down-Shift CsPbCl3:Mn Quantum Dots for Boosting the Efficiency and Stability of Perovskite Solar Cells. *ACS Energy Letters* 2, 1479–1486. doi: 10.1021/acsenergylett.7b00375

Wang, A., Yan, X., Zhang, M., Sun, S., Yang, M., Shen, W., et al. (2016). Controlled Synthesis of Lead-Free and Stable Perovskite Derivative Cs2SnI6 Nanocrystals via a Facile Hot-Injection Process. *Chemistry of Materials* 28, 8132–8140. doi: 10.1021/acs.chemmater.6b01329

Wang, H.-C., Wang, W., Tang, A. C., Tsai, H. Y., Bao, Z., Ihara, T., et al. (2017). High-Performance CsPb1-xSnxBr3 Perovskite Quantum Dots for Light-Emitting Diodes. *Angewandte Chemie-International Edition* 56, 13650–13654.

Wang, L., Shi, Z., Ma, Z., Yang, D., Zhang, F., Ji, X., et al. (2020). Colloidal Synthesis of Ternary Copper Halide Nanocrystals for High-Efficiency Deep-Blue Light-Emitting Diodes with a Half-Lifetime above 100 h. *Nano Letters* 20, 3568–3576. doi: 10.1021/acs.nanolett.0c00513

Wang, L., Pan, J., Liu, C., Zhao, Z., Fang, F., Wang, Y., et al. (2021). Tailoring Nanostructures of Quantum Dots toward Efficient and Stable All-Solution Processed Quantum Dot Light-Emitting Diodes. *ACS Appl Mater Interfaces*

Wang, L., Pan, J., Qian, J., Lei, W., Wu, Y., Zhang, W., et al. (2018). A highly efficient white quantum dot light-emitting diode employing magnesium doped zinc oxide as the electron transport layer based on bilayered quantum dot layers. *Journal of Materials Chemistry C* 6, 8099–8104. doi: 10.1039/c8tc03014f

Wang, L., Pan, J., Qian, J., Liu, C., Zhang, W., Akram, J., et al. (2019). Performance Enhancement of All-Inorganic Quantum Dot Light-Emitting Diodes via Surface Modification of Nickel Oxide Nanoparticles Hole Transport Layer. *ACS Applied Electronic Materials* 1, 2096–2102. doi: 10.1021/acsaelm.9b00479

Yang, B., Chen, J., Hong, F., Mao, X., Zheng, K., Yang, S., et al. (2017). Lead-Free, Air-Stable All-Inorganic Cesium Bismuth Halide Perovskite Nanocrystals. *Angewandte Chemie-International Edition* 56, 12471–12475. doi: 10.1002/anie.201704739

Yang, P., Liu, G., Liu, B., Liu, X., Lou, Y., Chen, J., et al. (2018). All-inorganic Cs2CuX4 (X = Cl, Br, and Br/I) perovskite quantum dots with blue-green luminescence. *Chem Commun (Camb)* 54, 11638–11641. doi: 10.1039/c8cc07118g

Yan, S., Li, Q., Zhang, X., Tang, S., Lei, W., Chen, J., et al. (2019). A vertical structure photodetector based on all−inorganic perovskite quantum dots. *Journal of the Society for Information Display* 28, 9–15. doi: 10.1002/jsid.853

Yu, H., Liu, X., Yan, L., Zou, T., Yang, H., Liu, C., et al. (2019). Enhanced UV–visible detection of InGaZnO phototransistors via CsPbBr3 quantum dots. *Semiconductor Science and Technology* 34

Zhang, M., Wang, L., Meng, L., and Zhong, H. (2018). Perovskite Quantum Dots Embedded Composite Films Enhancing UV Response of Silicon Photodetectors

for Broadband and Solar-Blind Light Detection. *Advanced Optical Materials* 6,

Zhang, X., Cao, W., Wang, W., Xu, B., Liu, S., Dai, H., et al. (2016). Efficient light-emitting diodes based on green perovskite nanocrystals with mixed-metal cations. *Nano Energy* 30, 511–516. doi: 10.1016/j.nanoen.2016.10.039

Zhang, J., Yang, Y., Deng, H., Farooq, U., Yang, X., Khan, J., et al. (2017). High Quantum Yield Blue Emission from Lead Free Inorganic Antimony Halide Perovskite Colloidal Quantum Dots. *Acs Nano* 11, 9294–9302. doi: 10.1021/acsnano.7b04683

Zhou, L., Xu, Y. F., Chen, B. X., Kuang, D. B., and Su, C. Y. (2018). Synthesis and Photocatalytic Application of Stable Lead-Free Cs2AgBiBr6 Perovskite Nanocrystals. *Small* 14, 189.

Conflict of Interest: CL was employed by the company China Nuclear Power Engineering Co., Ltd.

The remaining authors declare that the research was conducted in the absence of any commercial or financial relationships that could be construed as a potential conflict of interest.